# Testing and Characterization of Nano-structured Alumina Coating Prepared by Different Methods on Ti-6Al-4V alloy (Comparative Study)

**Suha Saadi, B.D.S.[1], Basima M.A. Hussain, B.D.S., M.Sc., Ph.D.[2]**

[1]M.Sc. Student. Department of Prosthodontics. College of Dentistry, University of Baghdad

[2]Assisstant Professor. Department of Prosthodontics. College of Dentistry, University of Baghdad

**Abstract:** _Introduction: Dental implant had become the most demanded alternative for tooth replacement. This study dealt with modification of Ti-6Al-4V alloy surface to be more compatible with surrounding tissue. Material and method: titanium discs were used (2 mm -10 mm in thickness and diameter respectively). The discs were divided in to four groups: A) control group of machined discs without surface modification; B) machined discs with physical and chemical vapor deposition(PVD-CVD) of alumina nano particles; C) laser ablated surface with physical and chemical vapor deposition(PVD-CVD) of alumina nano particles and D) machined discs coated with alumina nanoparticles by pulsed laser deposition(PLD). The surface characteristics were studied by scanning electron microscope, x-ray diffraction, atomic force microscope, optical microscope, wettability property (obtained after 15 sec and 30 sec), corrosion resistance (obtaining corrosion rate and tafel plot) and adhesion strength of coated discs. Results: SEM images showed nanofeatured alumina of the coated groups with distinct layering of alumina particles and signs of nanowires in LA-PVD-CVD group. XRD analysis shows α and δ pattern of alumina. Contact angle measurements of the four experimental groups in 15 and 30 sec show highly significant difference (P<0.01). Corrosion rate shows highly significant difference (P<0.01) between metal showed and alumina coated surfaces. Scratch test of the coated layer of the three experimental groups were highly significant difference (P<0.01) with the lowest adhesion in PVD-CVD and highest in LA-PVD-CVD. Conclusion: An improvement in corrosion resistance of coated surfaces over metal showed. The adhesion strength was improved by with laser ablation in PVD-CVD group while a decrease in wettability of alumina coated surfaces in comparison to uncoated surface._

**Keywords:** corrosion, wettability, scratch test, PVD-CVD, PLD

## 1. Introduction

The last century witnessed a great evolution in science, the great invention of dental implant had been noticed in dentistry. The biological fixation between the dental implant surface and jaw bone should be considered a basic factor for the long-term success of implant-supported prostheses, this is what is termed osseointegration[1]. The strategy of shortening the healing period after surgery and loading the implants with oral forces safely can be done by modification in the surgical technique, changing the implant design and altering the biocompatibility of titanium implant surface [2].

Aluminium oxide ($Al_2O_3$) is one of the most preferred oxides in industrial applications due to its superior properties. In addition to bulk form, alumina can be applied as a thin film for various applications including insulation corrosion protection and wear resistant surfaces [3].

Laser technique was used for surface modification of Ti-6Al-4V alloy to increase surface area and consequently increase surface roughness of titanium alloy to enhance adherence of thin film coating. It is cleaner and more biologically accepted method than using toxic chemical etchants and grit blast [4].

Deposition of nanostructure coatings by physical vapor deposition and/or chemical vapor deposition, had gained a great attention due to their unique physical and chemical properties, e.g. extremely high indentation hardness, excellent high temperature oxidization resistance with high corrosion, abrasion and erosion resistance [5][6].

Pulsed laser deposition process has the ability to control the interface layer between the thin film and the substrate material, and this will improve the film adhesion to substrate. Due to their versatility, controllability, uniform films deposition, with accurate control of the crystallinity and stoichiometry, it is considered as beneficial method for making thin films of functional biomaterials [7].

Studies had proved that the surface roughness of implant affects osseointegration as well as the mechanical stability of the dental implants [8][9].

The surface wettability, micro- and nano-topography, surface energy, surface charge and functional groups of a biomaterial determine the biological cascade of events at the implant-host interface that involves adsorption of protein, soft and hard-tissue interactions and formation of bacterial film [10]. Corrosion resistance, deterioration and corrosion debris are important parameters in selection of biomaterials. The intrinsic toxicity of these metallic ions (produced by corrosion of metals) are correlated with their ability to attach to macromolecules (host protiens). The tissue response depends on the concentration of corrosion products and their toxicity [2].

## 2. Material and method

### 2.1 Sample Preparation

Titanium alloy discs with (2mm, 10mm in thickness and diameter) were used, each disc was polished using aluminum oxide sandpaper sheets graduated from 400 to

2000. The discs were cleaned with deionized water then immersed in ethanol bath in ultrasonic cleaner for 15 minutes at 30°C and left to dry. The discs were divided in to four groups: the machined discs were used as control group, machined discs to be coated with alumina by PVD-CVD, laser ablated discs to be coated with alumina by PVD-CVD and machined discs to be coated with alumina by PLD.

## 2.2 Laser ablation procedure

The discs allocated for laser ablation were positioned in 2D holder (10 cm) distant from the lenses of laser machine, wavelength: 1064 nm; frequency: 6 H; pulse duration: 10 nanoseconds; energy: 700 mJ and pulse every 1 mm andthe spot size of laser beam was 0.6 mm [11].

## 2.3 Physical Vapor Deposition

The polished and laser ablated discs were then seeded with aluminum by physical vapor (PVD) method. The tungsten boat was filled with certain amount of aluminum fine powder 325 mesh, 44 μm, purity 99.5 %to deposit 600 nm of aluminum film according to Holland formula:

$$t = m / 2\, p\pi\, R^2 \qquad [12]$$

The diffusion pump was $10^{-6}$ mbar in the bell jar and the electrical power supply was allowed to pass to the boat gradually. As the electrical current reached to 200 Ampere, the evaporation started. After consumption of the aluminum powder, the alternative resistor, the diffusion pump and rotary pump were switched off respectively. The PVD system regained its atmospheric pressure in a suitable time.

## 2.4 Chemical Vapor Deposition

The aluminum coated discs (polished and laser ablated)were inserted in the chemical vapor deposition (CVD) machine. The argon gas with high purity (99.99 %) was allowed to flow at flow rate 140 sccm to purge out gases inside the reactor. The furnace was set at 950 ˚C with heating rate 40 ˚C/minute (ramp) for 2 hours in an ambient pressure [13]. After finishing the programmed period, the substrates were allowed to cool within the furnace with gradual decreasing in the argon flow rate.

## 2.5 Pulsed Laser Deposition

Alumina target should be prepared to be source of coating material. Certain amount of alumina powder fine silt 22 μm, purity 99.95% was compacted using pressing machine with the mold (diameter 21 mm), the pressure was (15 ton) and the resulted target was 3 mm in thickness which fixed on the target holder in the lower part.The discs were fixed in the substrate holder at the upper compartment of the PLD and the substrate-target distance was 4 cm. The diffusion vacuum was $3_x10^{-4}$mbar [14]. The substrate was heatedto 300°C. The laser machine parameters were as follow: energy: 800 mJ, number of pulses: 500 pulses, frequency: 2 Hz and wavelength: 532 nm. The alumina target was bombed out by the laser machine in 45° angle and 10 cm distance from the target. As the pulses reached to the desired number (500 pulse), we slowly decreased the temperature of the lamb and the pressure inside the bell jar.

## 2.6 Surface Characterization

### 2.6.1 Scanning electron microscope
The control and experimental groups were imaged using SIGMA FE-SEM at 26.00 kV.

### 2.6.2 X-ray diffraction
The control and experimental groups were tested for surface structural analysis by SHMADZU-XRD-6000 using Cu target, voltage = 40.0 (kV) and current = 30.0 (mA). The 2θ angles were with scan range between 20-80°.

### 2.6.3 Surface roughness
The control and experimental groups were examined for surface roughness by Compact AFM NANO-PHYWE.

### 2.6.4 Optical microscope
Optical microscopic imaging was done to identify the surface layer of the control and experimental groups usingoptical microscope (OLYMPUS U- SPT-JAPAN).

### 2.6.5 Contact angle measurement
The wettability of the control and experimental groups was tested by Contact Angle Meter Series using Hank buffered salt solution that fills the syringe.The sample was positioned on a flat movable tray. The syringe was released carefully to allow for dropping the fluid on the substrate. The contact angle was measured from both sides within 15 and 30 seconds intervals and the average contact angle of right and left sides was obtained for each interval period.

### 2.6.6 Corrosion test
The corrosion behavior was tested by Digi-Ivy. The liquid used was freshly prepared Hank buffered salt solution, that composed ofNaCl, KCl, $CaCl_2$, $MgSO_4$, $NaH_2PO_4$, $NaHCO_3$, GLUCOSE, $K_2HPO_4.3H_2O$, and $MgCl_2.6H_2O$ that dissolved in distilled water immediately prior to use. The glass baker was filled with 50 mL of freshly prepared Hank solution. The disc was attached to the working electrode, the counter electrode was platinum electrode and the reference electrode were all immersed in hank solution. The initial and final potential were obtained from open circuit potential which is -2 mV and scanning rate was 10 mV/sec. Tafel plot were obtained and the corrosion rate of each group were measured.

### 2.6.7 Scratch test
Macro and micro tests were performed through scratch testing. The device within the range of critical forces 1N to 200N. The tester is compatible with ASTM Standard C1624 (C1624-05) [15], ISO International standards 20502 [16] and EN European Standard 1071-3 [17]. From this system we obtained the data of critical force (Fc). The normal load at which failure happens is called the critical normal load. It is generally accepted that the test is suitable for coatings of thickness ranging from 0.1 to 20 μm.

## 3. Results

### 3.1 SEM

Scanning electron microscopical images of the experimental groups are shown in figure (1). The control group (1.A)

shows no distinct features with transverse lines expressing polishing of the discs. The figure (1.B) shows laser ablation of the discs with distinct cracks the nanopits. The PVD-CVD on polished surface is expressed in figure (1.C) showing distinct crystal like structure of alumina with different sizes due to coherence of the crystals. The figure (1.D) is laser ablated surface with combination PVD-CVD showing larger clusters of crystal than in figure (1.C) with sign of nanowire structures within the crystal. Figure (1.E) shows pulsed laser deposition on polished surface with apparent crystal structure of alumina with different diameters and no distinctive structure.
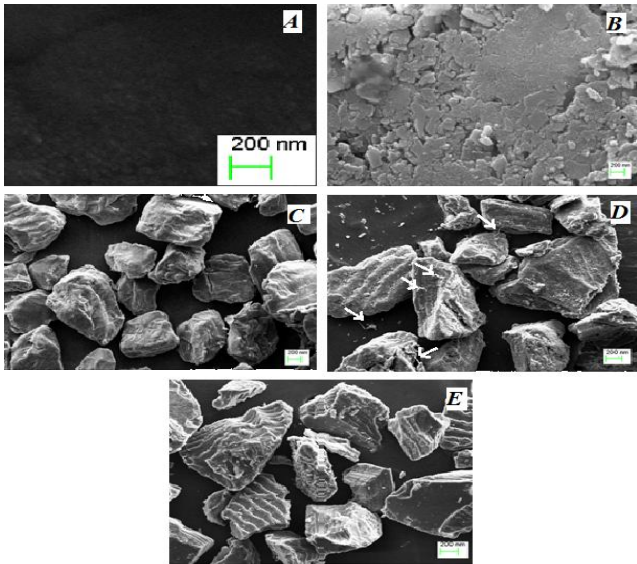


**Figure 1:** SEM of experimental groups, A: control group; B: laser ablated surface; C: PVD-CVD of alumina on polished surface; D: PVD-CVD of alumina on laser ablated surface; and E: PLD of alumina on polished surface.

### 3.2 XRD analysis

XRD of control, PVD and CVD are shown in figure (2). The control group with distinctive titanium pattern (100)(002)(101)(102)(201) with reflection peak at $2\theta=$ 35.09, 38.42, 40.17, 53.004, 77.36 respectively. The polished discs coated with aluminum by PVD shows titanium pattern in addition to aluminum pattern. Aluminum pattern (200)(220) at $2\theta=$ 44.83 and 65.18 respectively. The polished surface coated by PVD-CVD shows $\alpha$ alumina pattern (125)(1010) at $2\theta=$ 70.41 and 76.86 respectively as well as $\delta$ alumina pattern (523) at $2\theta=$ 63.88.
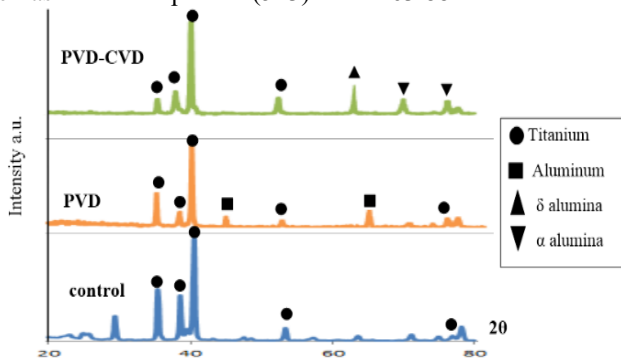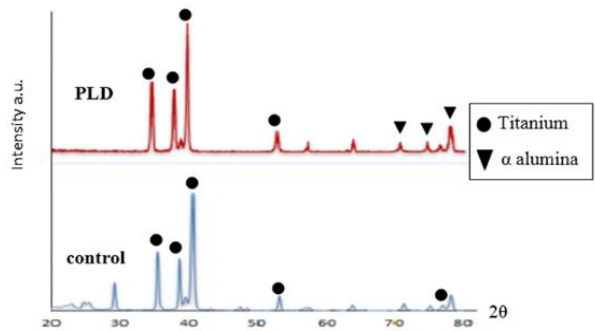


**Figure 2:** XRD pattern of control group, PVD coating and PVD-CVD coating on machined surface

Figure (3) shows, in addition to control group, laser ablated surface with unchanged chemical structure with the same titanium pattern of control but with decreased intensity in addition to titanium pattern (200)(112) with reflection peak at $2\theta=$ 74.15, 76.21, respectively. Laser surface surface coated with aluminum by PVD shows aluminum pattern (200)(220) at $2\theta=$ 44.83 and 65.18 respectively. The laser ablated surface coated by PVD-CVD shows $\alpha$ alumina (125)(208)(119) at $2\theta=$ 70.41, 74.29 and 77.54 respectively and $\delta$ alumina (2212)(523) at $2\theta=$ 57.40 and 63.88 respectively.
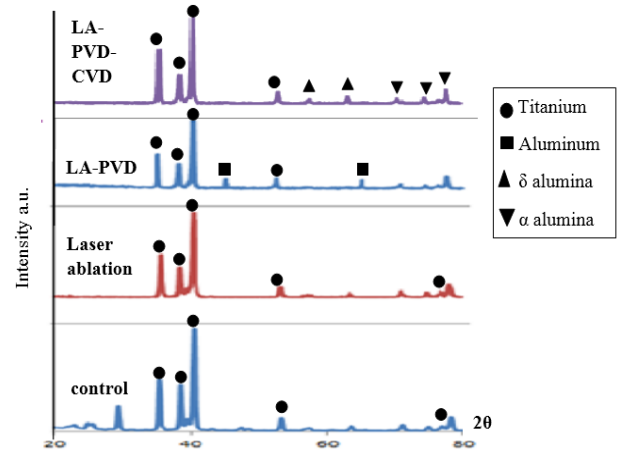


**Figure 3:** XRD pattern of control group, laser ablated surface, PVD coating and PVD-CVD coating on laser ablated surface

Figure (4) shows XRD pattern of control group and PLD group. The PLD group shows $\alpha$ alumina (125)(208)(119) at $2\theta=$ 70.41, 74.29 and 77.54 respectively.



**Figure 4:** XRD pattern of control group and PLD coating on machined surface

### 3.3 Roughness measurement

AFM topography was taken for all experimental groups as shown in figure (5). The machined group in figure (5.A) shows rough surface caused by polishing of the discs. The laser ablated surface in figure (5.B) shows distinct hole representing the area of incidence of laser beam. Figure (5.C and D) representing PVD coated on machined surface and laser ablated surface with distinct nano peaks with thicker diameter nano peaks in laser ablated-PVD coating. Figure (5.E and F) representing PVD-CVD on machined and laser ablated surface representing thinning in nano-structures. The PLD group are shown in figure (5.G), with thin nano peaks.
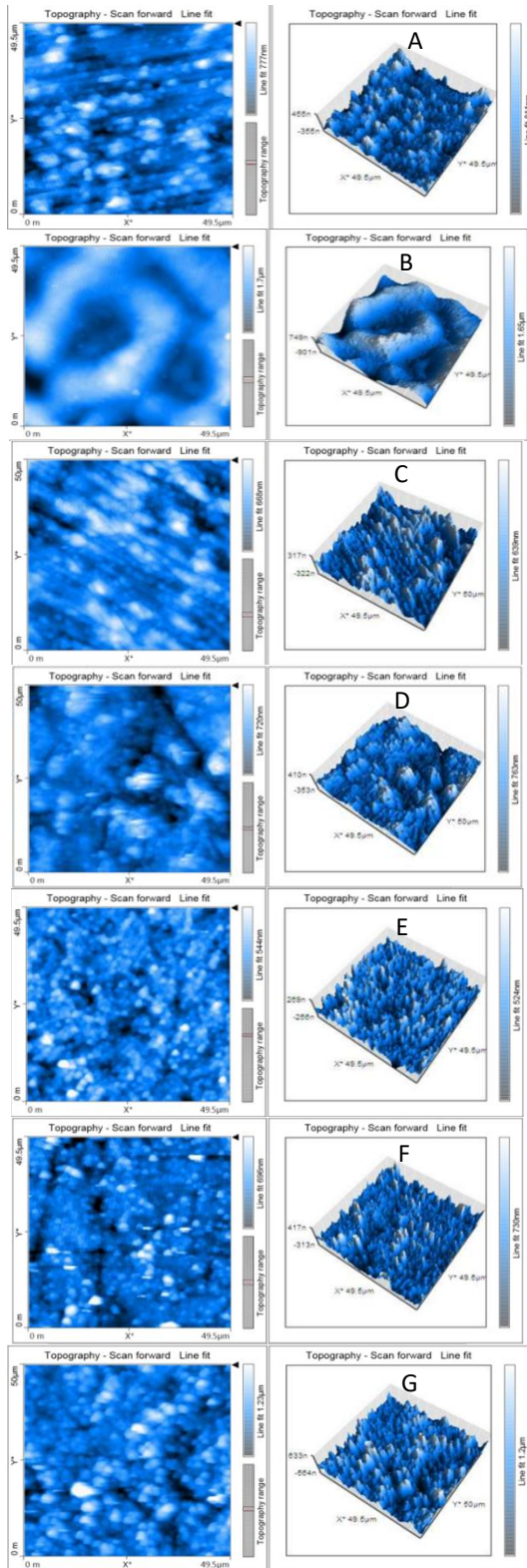
**Figure 5:** AFM topography of test groups, A: machined surface; B: laser ablated surface; C: aluminum deposited on machined surface by PVD; D: aluminum deposited on laser ablated surface by PVD; E: alumina deposited on machined surface by CVD; F: alumina deposited on laser ablated surface by CVD; G: alumina deposited by PLD

**Table 1:** AFM values of test groups

| Group | Average Roughness (nm) | Average Grain size (nm) | Thickness measurement (nm) |
|---|---|---|---|
| Control group | 55.865 | 323.78 | - |
| Laser ablated surface | 92.7 | 105.45 | - |
| PVD on untreated surface | 110.13 | 654.44 | 474.92 |
| PVD on laser ablated surface | 115.96 | 702.76 | 506.23 |
| PVD-CVD | 83.253 | 512.63 | 585.12 |
| LA-PVD-CVD | 110.41 | 678.08 | 631.19 |
| PLD | 199.36 | 524.33 | 672.6 |

### 3.4 Contact angle measurement

Contact angle imaging of the four experimental groups at two interval periods (15 and 30 sec) are shown in figure (6).
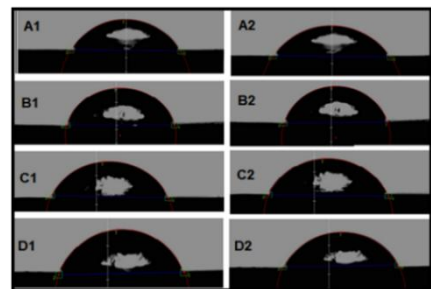


**Figure (6)** Contact angle A1: control group (15 sec), A2: control group (30 sec), B1: PVD-CVD (15 sec), B2: PVD-CVD (30 sec), C1: laser ablation PVD-CVD(15 sec), C2: laser ablation PVD-CVD(30 sec), D1: PLD at(15 sec), D2: PLD(30 sec)

Descriptive statistics of contact angle for the experimental groups, the non-modified surface (control group), the PVD-CVD, LA-PVD-CVD and PLD, for two testing periods 15 sec and 30 second are shown in the table (2). The mean values of the four experimental groups at 15 and 30 sec intervals were then tested using ANOVA showing that there is highly significant difference ($P<0.01$) at three degrees of freedom of wettability with different surface treatment procedures as shown in table (3). To differentiate between equality of mean value of the four test groups, we used LSD test, showing that there is highly significant difference among test groups at each interval as shown in table (2).

**Table 2:** Mean ($\pm$ SD) of contact angle for tested groups and coating methods

| The group | No. | Mean $\pm$ SD | |
|---|---|---|---|
| | | *15 Sec.* | *30 Sec.* |
| Control | 5 | 51.88° $\pm$ 3.72 c | 48.71° $\pm$ 3.02 c |
| PVD-CVD | 5 | 77.02° $\pm$ 3.46 a | 74.31° $\pm$ 3.53 a |
| LA-PVD-CVD | 5 | 73.54° $\pm$ 3.44 ab | 71.91° $\pm$ 2.53 ab |
| PLD | 5 | 71.95° $\pm$ 2.69 b | 69.42° $\pm$ 3.92 b |
| LSD value | | 4.494 ** | 4.419 ** |
| P-value | | 0.0001 | 0.0001 |
| ** ($P<0.01$). | | | |

**Table 3:** ANOVA test of contact angle in 15 and 30 sec

|  | Sources | Sum of Squares | Df | Mean Square | F value | Pr > F |
|---|---|---|---|---|---|---|
| *15 sec* | Model | 2072.061 | 3 | 690.687 | 63.568 | <.0001 |
|  | Error | 173.845 | 16 | 10.865 |  |  |
|  | Corrected Total | 2245.906 | 19 |  |  |  |
| *30 sec* | Model | 1930.91 | 3 | 643.637 | 57.273 | <.0001 |
|  | Error | 179.808 | 16 | 11.238 |  |  |
|  | Corrected Total | 2110.718 | 19 |  |  |  |

On the other hand, we compared each group for two interval periods (15 sec and 30 sec) separately using paired T test. The **P values≥ .01** for control group, LA-PVD-CVD and PLD and significant difference in PVD-CVD groups **P ≤ .01.**

**Table 4:** Paired Samples Correlations of contact angle

| Group | N | Correlation | Sig. |
|---|---|---|---|
| control | 5 | .707 | .182 |
| PVD-CVD | 5 | .981 | .003 |
| LA-PVD-CVD | 5 | .883 | .047 |
| PLD | 5 | .956 | .011 |

**Table 5:** Paired Samples Test of Contact Angle in 15-30 sec

| Group | Paired Differences | | | | | T | df | Sig.(2-tailed) | Corr. |
|---|---|---|---|---|---|---|---|---|---|
|  | Mean | S.D. | S.E. Mean | 95% Confidence Interval of the Difference | | | | | |
|  |  |  |  | Lower | Upper | | | | |
| CONTROL | 3.166 | 2.66 | 1.19068 | -.13985- | 6.47185 | 2.659 | 4 | .056 | .328 |
| PVD-CVD | 2.718 | .689 | .30824 | 1.86218 | 3.57382 | 8.818 | 4 | .001 | .987 |
| LA-PVD-CVD | 1.632 | 1.69 | .75777 | -.47190- | 3.73590 | 2.154 | 4 | .098 | .999 |
| PLD | 2.528 | 1.566 | .70071 | .58252 | 4.47348 | 3.608 | 4 | .023 | .973 |

### 3.5 Potentiostat test

The four experimental groups are tested using potentiostat test for corrosion behavior. Each group was imaged by optical microscope as seen in figure (8). Figure (8.A2) shows area of micropits distributed on the surface of uncoated surface. Figure (8.B,C and D) show small areas of uncoated surfaces of the experimental alumina coated surfaces.
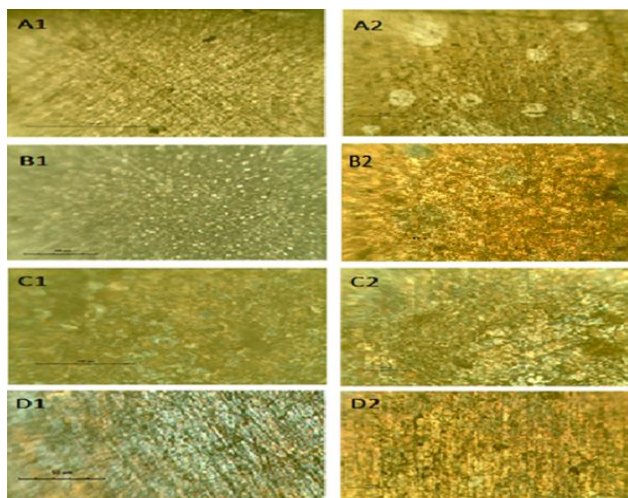


**Figure 8:** Optical microscopical image of discs before and after corrosion. A1: uncoated surface before corrosion; A2: uncoated surface after corrosion; B1: PVD-CVD before corrosion; B2: PVD-CVD after corrosion; C1: LA-PVD-CVD before corrosion; C2: la- PVD-CVD after corrosion; D1: PLD before corrosion D2: PLD after corrosion

### 3.5.1 Potentiodynamic polarization curves
The tafel plot was used to estimate the corrosion behavior in relation to potential and current. The higher polarization voltage and lower current density indicates better resistance to corrosion. The tafel plot in table shows lower polarization voltage of control group and higher current density in relation to coated group by different methods, table (6).
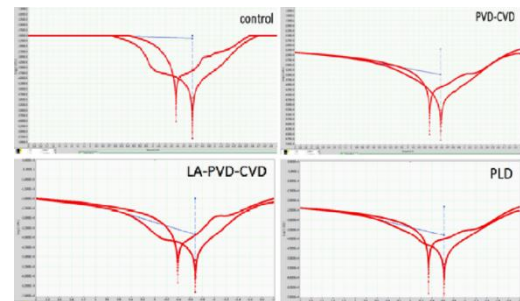


**Figure 9:** tafel plot of experimental groups

**Table 6:** effect of group on polarization valtage and current density

| Group | Polarization voltage (V) | Current density (A/cm²) |
|---|---|---|
| Control | -0.683 | 1.2E-5 |
| PVD-CVD | -0.582 | 5.23E-6 |
| LA-PVD-CVD | -0.678 | 6.53E-6 |
| PLD | -0.619 | 4.91E-6 |

### 3.5.2 Corrosion rate
Descriptive statistics of the experimental groups are shown in table (7).The equality of means was tested by ANOVA and shown in table (8) that there is significant difference among test groups P≤ .01 at three degrees of freedom.LSD was used to differentiate the test groups and found that there is significant difference between control group and coated surfaces whereas no significant difference between the three experimental coated groups.

**Table 7:** Comparison between different groups in Corrosion rate

| The group | No. | Mean ± SD of Corrosion rate |
|---|---|---|
| Control | 5 | 2.86 E-1 ± 0.75 a |
| PVD-CVD | 5 | 1.526 E-1± 0.29 b |
| LA-PVD-CVD | 5 | 1.832 E-1 ± 0.63 b |
| PLD | 5 | 1.648 E-1 ± 0.58 b |
| LSD value | --- | 0.792 ** |
| P-value | --- | 0.0099 |
| ** (P<0.01). | | |

**Table 8:** ANIOVA test of corrosion rate

| Source | Sum of Squares | df | Mean Square | F value | Pr > F |
|---|---|---|---|---|---|
| Model | 5.560 | 3 | 1.853 | 5.307 | .010 |
| Error | 5.587 | 16 | .349 | | |
| Corrected Total | 11.147 | 19 | | | |

### 3.6 Adhesion strength

Adhesion strength of alumina thin film deposited Ti-6Al-4V disc by PVD-CVD, LA-PVD-CVD and PLD was tested by scratch test. Optical image was taken for each group as shown in figure(10).
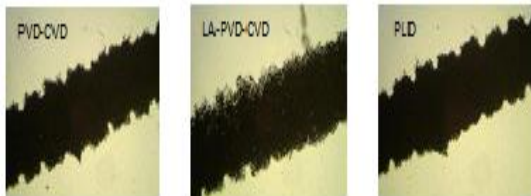


**Figure 10:** Microscopical image of scratching surface of thin film coating

Table (9) shows descriptive statistics of the critical force for the three experimental groups: PVD-CVD, LA-PVD-CVD and PLD. The equality of means was tested by ANOVA, table (10), that shows a significant difference among the three test groups P≤ .01 at two degrees of freedom.LSD was used to differentiate the test groups, which shows highly significant difference between each experimental group.

**Table 9:** Comparison between different groups in Scratch test

| The group | No. | Mean ± SD of Scratch test |
|---|---|---|
| PVD-CVD | 10 | 6.60 N ± 0.53 c |
| LA-PVD-CVD | 10 | 9.25 N ± 1.01 a |
| PLD | 10 | 8.30 N ± 0.00 b |
| LSD value | --- | 0.599 ** |
| P-value | --- | 0.0001 |
| ** (P<0.01). | | |

**Table 10:** ANOVA test for critical force

| Source | Sum of Squares | df | Mean Square | F value | Pr > F |
|---|---|---|---|---|---|
| Model | 36.05 | 2 | 18.025 | 42.23 | <.0001 |
| Error | 11.525 | 27 | .427 | | |
| Corrected Total | 47.575 | 29 | | | |

## 4. Discussion

Untreated surface of Ti-6Al-4V was shown to possess the lowest contact angle when compared to test groups. This may be related to the fact that alumina nanoparticle deposition may shift the material to be more hydrophobic with increase surface roughness in addition to the difference in surface chemistry between titanium alloy and alumina and this is agreed with [18]. The combination PVD-CVD and PLD methods are approximated the results obtained by [19] who deposited alumina by atomic layer deposition. An obvious decrease in contact angle in this experiment in comparison to deposition by nanoporous anodic alumina mentioned by [20].This study revealed an increase in contact angle with increase in surface roughness, and seems to be sensitive to the method of surface treatment and this is agreed with [21].

The control group exhibits the highest corrosion rate in comparison to coated surfaces. This may be explained that Ti-6Al-4V alloy is composed of different elements (Al and V) and to the more defective nature of grown passive layers and the increased reactivity of alloy and this is agreed with [22].The coated surfaces with alumina show high corrosion resistance to metallic implant surfaces due to its excellent mechanical properties and chemical stability and biocompatibility as stated by[23]. The combination PVD-CVD processes on machined and laser ablated surface reveal more resistance to corrosion than uncoated surface. This may be related to chemical stability of alumina and good adherence of the thin film to Ti-6Al-4V alloy and this is agreed with [24]. An improvement in corrosion resistance was shown in PLD group due to to good adherence to Ti-6Al-4V alloy and the negligible pores and cracks in the alumina thin film that is agreed with [25][26].

The combination of PVD-CVD methods show good adhesion of alumina thin film to Ti-6Al-4V alloy, which is the force causing failure of the material and detachment from the substrate and this is related to deposition method of combined PVD-CVD that possess good adhesion properties and this is agreed with [27].The adhesion strength of alumina coated by PVD-CVD increases with increasing interlocking surface area done by laser ablation of titanium surface in addition to deposition properties of PVD-CVD made it possess the highest adhesion strength among experimental groups and this is agreed with [4].PLD also shows good adhesion of alumina to titanium alloy substrates which is the main advantage of this method. This is might be due to heating substrate during deposition and the plasma created from ablation of alumina target is heated to a very high temperature resulted in inclusion of it to substrate surface and this is agreed with [28].

## 5. Conclusion

The most attractive coating procedures are PVD, CVD and PLD due to high adherence of thin film and consequently improvement in corrosion resistance. Coating procedure to Ti-6Al-4V may change wettability to decrease hydrophilicity of the surface.

## References

[1] Novaes Jr., Arthur Belém; de Souza, Sérgio Luis Scombatti; de Barros, Raquel Rezende Martins; Pereira, Karina Kimiko Yamashina; Iezzi, Giovanna; Piattelli, Adriano(2010). Influence of Implant Surfaces on Osseointegration.Braz Dent J, 21(6): 471-481.

[2] Elias C.N (2011). Factors Affecting the Success of Dental Implants. Edited by Ilser Turkyilmaz, ISBN 978-953-307-658-4.

[3] Miró, Marina Martinez (2012).Topographical Control and Characterization of Al/Al2O3Nanowire Coatings for Improved Osseointegration of Implant Materials.

[4] Palmieri F.L, Watson KA, Morales G,Williams T, Hicks R, Wohl C.J, Hopkins J.W, Connell J.W.(2012).Laser ablation surface preparation of Ti-

6Al-4V for adhesive bonding. ACS applied materials & interfaces 5 (4), 1254-1261

[5] Zou, H., Zhou, L., Li, Y., Cui, Y., Zhong, H., Pan, Z., Yang, Z., and Quan, J. (2010) Benzo[e]isoindole-1,3-diones as Potential Inhibitors of Glycogen Synthase Kinase-3 (GSK-3). Synthesis, Kinase Inhibitory Activity, Zebrafish Phenotype, and Modeling of Binding Mode. J Med Chem 53(3): 994-1003.

[6] Chen, Daniel; Mocker, Martin; Preston, David S.; and Teubner, Alexander. 2010. "Information System strategy: Reconceptualization, Measurement, and Implications,"MIS Quarterly, (34:2) pp.233-259.

[7] Carradò, Adele; Pelletier, Hervé and Roland , Thierry (2011). Nanocrystalline Thin Ceramic Films Synthesised by Pulsed Laser Deposition and Magnetron Sputtering on Metal Substrates for Medical Applications, Biomedical Engineering - From Theory to Applications, Prof. Reza Fazel (Ed.), ISBN: 978-953-307-637-9.

[8] Werner S, Huck O, Frisch B, Vautier D, Elkaim R, Voegel JC, Brunel G Tenenbaum H. (2009). The effect of microstructured surfaces and laminin-derived peptide coatings on soft tissue interactions with titanium dental implants. Biomaterials. Vol.30, pp.2291-2301.

[9] Zhu X, Chen J, Scheideler L, Reichl R, Geis-Gerstorfer J. (2004). Effects of topography and composition of titanium surface oxides on osteoblast responses. Biomaterials. Vol.25, pp.4087-4103.

[10] Kohavi D, Badihi HL, Rosen G, Steinberg D, Sela MN (2013). Wettability versus electrostatic forces in fibronectin and albumin adsorption to titanium surfaces. Clin Oral Implants Res;24(9):1002–8

[11] Oliveira V., Ausset S., Vilar R. Surface micro/nanostructuring of titanium under stationary and non-stationary femtosecond laser irradiation, Appl. Surf. Sci. 255 (2009) 7556-7560.

[12] Holland L.(1996). "Vacuum Deposition of Thin Films", Chapman and Hill LTD., London.

[13] Zhang, Yong, Li, Ruying, Zhou, Xiaorong, Cai, Mei, and Sun, Xueliang. Selective Growth of α-Al2O3 Nanowires and Nanobelts. Journal of Nanomaterials Volume 2008, Article ID 250370, 8 pages

[14] Balakrishnan G., Kuppusami P., Tripura Sundari S., Thirumurugesan R., Ganesan V., Mohandas E., Sastikumar D (2009).Structural and optical properties of γ-alumina thin films prepared by pulsed laser deposition. Thin Solid Films.

[15] ASTM International, Standard C1624 (C1624-05): Test Method for Adhesion Strength and Mechanical Failure Modes of Ceramic Coatings by Quantitative Single Point Scratch Testing, Conshohocken, 2005.

[16] ISO copyright office, International standards ISO 20502: Fine ceramics (advanced ceramics, advanced technical ceramics) – Determination of adhesion of ceramic coatings by scratch testing, Geneva, 2005.

[17] EN 1071-3, Advanced technical ceramics – Method of test for ceramic coatings – Part 3: Determination of adhesion and other mechanical failure modes by a scratch test, Brussels, 2006.

[18] Rangharajan K.K., Kwak K.J, Conlisk A.T., Wu Y, Prakash S. (2015). Effect of surface modification on interfacial nanobubble morphology and contact line tension. Soft Matter,11, 5214-5223

[19] Li Hui-Ying, Liu Yun-Fei, Duan Yu, Yang Yong-Qiang and Lu Yi-Nan (2015). Method for Aluminum Oxide Thin Films Prepared through Low Temperature Atomic Layer Deposition for Encapsulating Organic Electroluminescent Devices. Materials, 8, 600-610.

[20] Kumeria Tushar, Santos Abel, Losic Dusan (2014). Nanoporous Anodic Alumina Platforms: Engineered Surface Chemistry and Structure for Optical Sensing Applications. Sensors, 14, 11878-11918.

[21] Tasaltin Nevin, Sanli Deniz, Jonáš Alexandr, Kiraz Alper and Erkey Can (2011). Preparation and characterization of superhydrophobic surfaces based on hexamethyldisilazane-modified nanoporous alumina. Nanoscale Research Letters 6:487.

[22] Ali Hanan, Saleem Shatha, Al-Zubaydi Thair L (2014). Evaluation of corrosion behavior of bioceramics coated commercially pure titanium and Ti-6Al-4V alloy. J Bagh College Dentistry Vol. 26(3).

[23] Zykova A, Vladimir S , Anna Y, Leonid S , Renata R , Jerzy S, Stas Y (2015). Formation of Solution-derived Hydroxyapatite Coatings on Titanium Alloy in the Presence of Magnetron-sputtered Alumina Bond Coats. The Open Biomedical Engineering Journal; 9(Suppl 1-M16): 75-82.

[24] Lukaszkowicz, Krzysztof (2011). Review of Nanocomposite Thin Films and Coatings Deposited by PVD and CVD Technology, Nanomaterials, Prof. Mohammed Rahman (Ed.), ISBN: 978-953-307-913-4

[25] Sujaya C and Shashikala H.D(2012). Hardness and electrochemical behavior of ceramic coatings on CP titanium by Pulsed laser deposition

[26] Popescu-Pelin G., Craciun D., Socol G., Cristae D., Florian L., Badea M., Socol M., Craciun V (2015). Investigation of pulsed laser deposited TiN thin films for titanium implants. Romanian Reports in Physics, Vol. 67, No. 4, P. 1491-1502.

[27] Mathur Sanjay, Shen Hao and Altmayer Jessica (2007). Nanostructure functional ceramic coatings by molecule-based chemical vapor deposition. Rev.Adv.Mater.Sci. 15, 16-23

[28] Johnson Shevon(2005). Pulsed laser deposition of hydroxyl apatite thin films.